

# Computational Implications of Lognormally Distributed Synaptic Weights

*This paper reviews some important, recent works on computation with sparsely distributed synaptic weights, and discusses possible implications of the synaptic principle of neural computation by spiking neurons, with potential applications in neuromorphic engineering.*

By JUN-NOSUKE TERAMAE AND TOMOKI FUKAI

**ABSTRACT** | The connectivity structure of neural networks has significant implications for neural information processing, and much experimental effort has been made to clarify the structure of neural networks in the brain, i.e., both graph structure and weight structure of synaptic connections. A traditional view of neural information processing suggests that neurons compute in a highly parallel and distributed manner, in which the cooperation of many weak synaptic inputs is necessary to activate a single neuron. Recent experiments, however, have shown that not all synapses are weak in cortical circuits, but some synapses are extremely strong (several tens of times larger than the average weight). In fact, the weights of excitatory synapses between cortical excitatory neurons often obey a lognormal distribution with a long tail of strong synapses. Here, we review some of our important and recent works on computation with sparsely distributed synaptic weights and discuss the possible implications of this synaptic principle for neural computation by spiking neurons. We demonstrate that internal noise emerges from long-tailed distributions of synaptic weights to produce stochastic resonance effect in the reverberating synaptic pathways constituted by strong synapses. We show a spike-timing-dependent plasticity rule and other mechanisms that

produce such weight distributions. A possible hardware realization of lognormally connected networks is also shown.

**KEYWORDS** | Associative memory (AM); feedforward networks; network connectivity; neural dynamics; neuromorphic engineering; principal component analysis (PCA); recurrent networks; sparse coding; spike sequence; spike-timing-dependent plasticity (STDP); stochastic resonance

## I. INTRODUCTION

Much effort has been made to clarify the connectivity structure of cortical networks [1]–[4], and these anatomical or electrophysiological studies have shown that both connectivity patterns and link weights of cortical neural networks are highly nonrandom. For instance, the connectivity patterns of cortical networks deviate significantly from those of random networks, exhibiting an excess amount of network motifs consisting of a small number of densely connected neurons [5], [6]. Furthermore, recent electrophysiological studies have revealed that the amplitudes of excitatory–postsynaptic potentials (EPSPs) between cortical neurons are not distributed as Gaussian but are distributed as lognormal [6]–[10], implying that some synapses are very strong while many synapses are weak. For instance, Song *et al.* found significantly more connections with strengths above 1 mV than expected by best exponential or normal fit in rat visual cortex [6] ( $p < 0.0001$ , where  $p$  is the probability to have such observations from the null distributions). The same data set was best fit by a lognormal distribution. In CA3 area of the hippocampus [8], the weakest half of excitatory synapses contributed only 17% of the

Manuscript received August 16, 2013; revised January 28, 2014; accepted January 30, 2014. Date of publication March 14, 2014; date of current version March 25, 2014. The modeling studies were supported in part by the Japan Science and Technology Agency (JST) under the CREST program and the PRESTO program under Grants-in-Aid for Scientific Research (KAKENHI) 24120524 25430028 (to J. Teramae), and 22115013 (to T. Fukai).

**J. Teramae** is with the Graduate School of Information Science and Technology, Osaka University, Suita, Osaka 565-0871, Japan.

**T. Fukai** is with the RIKEN Brain Science Institute, Wako, Saitama 351-0198, Japan (e-mail: tfukai@riken.jp).

Digital Object Identifier: 10.1109/JPROC.2014.2306254

0018-9219 © 2014 IEEE. Personal use is permitted, but republication/redistribution requires IEEE permission. See [http://www.ieee.org/publications\\_standards/publications/rights/index.html](http://www.ieee.org/publications_standards/publications/rights/index.html) for more information.

total synaptic conductance, whereas the strongest 20% contributed 52%. A lognormal distribution, but not Gaussian, could account for such strong differences in the strength of individual synapses. Because strong synapses are sparse and weak synapses are dense, we may regard neural networks with lognormal weight distributions as “strong-sparse and weak-dense” (SSWD) networks [11], [12]. Evidently strong synapses are more effective in propagating spikes to downstream neurons, though such synapses are rare. In contrast, individual weak synapses are not powerful enough to activate downstream neurons, but they are very dense.

Then, a question arises: Are only strong synapses important for information processing? Are weak synapses unnecessary for creating network functions? Uncovering the functional implications of network links with extremely different strengths may furnish new insights into the circuit mechanism of computation by the brain. Moreover, recent progresses in supercomputing technologies and neuromorphic engineering [13] increase the relevance of realistic network models of spiking neurons. Therefore, understanding the dynamics of neural networks has great possibilities in the future development of brain-style computing systems. In this paper, we discuss recent experimental and theoretical results about the roles of strong and weak synapses for the dynamics and function of neural networks. Furthermore, we discuss how possibly lognormal distributions of synaptic weights appear in neural networks in an activity-dependent manner, and how such novel learning rules may contribute to computation in single neurons and neural networks.

## II. LOGNORMAL WEIGHT DISTRIBUTIONS

Lognormal EPSP distributions have been found between pyramidal neurons (i.e., the major type of cortical excitatory neurons) in rodent neocortex [6], [7], [10] and hippocampus [8]. Spine volumes were also suggested to obey lognormal distributions [14], [15]. To elucidate the basic computational function of lognormal weight distributions, we model a single neuron receiving random spike inputs at AMPA receptor-mediated synapses obeying such an EPSP distribution. Here, AMPA synapses are a class of excitatory synapses that mediate a fast glutamatergic synaptic current in the brain. Then, we connect such neuron models into two types of recurrent networks to see whether the results shown in single neurons are also valid in neural circuits.

### A. Lognormal EPSP Distributions in Neocortex and Hippocampus

Fig. 1(a) schematically illustrates an experimentally observed distribution of EPSPs ( $x$ ) measured from the

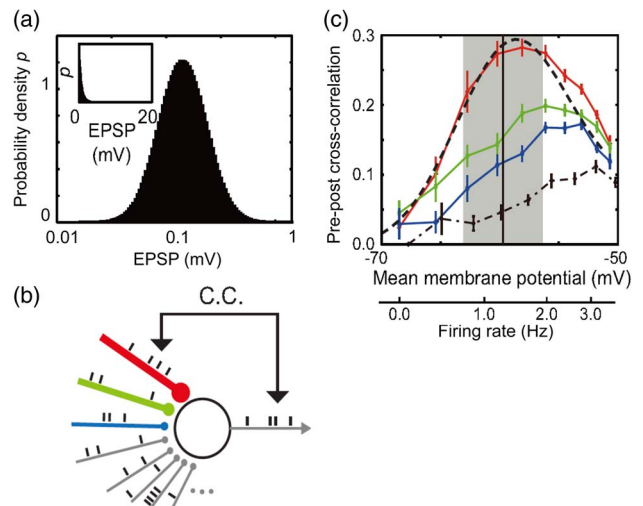


**Fig. 1. Stochastic resonance effects on neural firing by lognormal weight distributions. Modified from [11]. (a) The lognormal distribution of experimentally measured EPSP amplitudes is shown [6]. Inset plots the same distribution in the normal scale. We used this distribution in the present simulations of spiking neurons. (b) Schematic illustration of numerical simulations performed on a single integrate-and-fire neuron. (c) Coherence between output and input to the strongest synapse was calculated by numerical (solid) or analytical (dashed) methods as a function of input spike rate, or equivalently, the mean membrane potential. Colors indicate synaptic inputs in (b). A similar curve was calculated for the strongest synapse of Gaussian-distributed EPSP amplitudes (dotted-dashed line).**

resting potential, which is described as a lognormal distribution

$$p(x) = \frac{\exp[-(\log x - \mu)^2 / 2\sigma^2]}{\sqrt{2\pi}\sigma x}. \quad (1)$$

In this distribution, a minority of EPSPs between cortical excitatory neurons can be as large as several millivolts, while the majority are weak ( $< 1$  mV). For example, the amplitude of the largest EPSPs can be as big as 10 mV, which is much larger than the typical amplitude  $0.1 \sim 1$  mV of EPSPs of cortical synapses. Note that a large EPSP in a neuron pair may be mediated by multiple synaptic contacts between the pair. The lognormal distribution typically shows a long tail of strong synaptic weights. In fact, the coexistence of a small number of extremely strong connections and a large number of weak or modestly strong connections is important for what we show below, but whether the precise shape of weight distributions is lognormal is not crucial. In many cases, we could replace a lognormal weight distribution with a combination of a Gaussian weight distribution and several very strong connections. Therefore, the long-tailed feature is essential, but the exact lognormality is not really important.

## B. Lognormal Weight Distributions Induce Stochastic Resonance

The impact of a presynaptic spike at a strong synapse, which typically is as large as several millivolts, may amount to almost half of the gap between the resting membrane potential ( $-70$  mV) and firing threshold ( $-50$  mV). In this section, we show that the functional implication of such long-tailed weight distributions for neural information processing may be noise genesis on the membrane potential dynamics of single neurons [11], [12]. Implications of such noise genesis in network dynamics and network-level computation will be shown later. We performed most of the simulations presented in this paper using the following leaky integrate-and-fire model:

$$\frac{dv}{dt} = -\frac{1}{\tau_m}(v - V_L) - g_E(v - V_E) - g_I(v - V_I) \quad (2)$$

where  $v$  is the membrane potential and the second and third terms on the right-hand side represent conductance-based excitatory and inhibitory synaptic inputs, respectively. The excitatory and inhibitory synaptic conductances  $g_E$  and  $g_I$  normalized by the membrane capacitance obey

$$\frac{dg_X}{dt} = -\frac{g_X}{\tau_s} + \sum_j G_{X,j} \sum_{s_j} \delta(t - s_j - d_j), \quad X = E, I \quad (3)$$

where  $\delta(t)$  is the delta function; and  $G_j$ ,  $d_j$ , and  $s_j$  are the weight, delay, and spike timing of synaptic input from the  $j$ th neuron, respectively. The values of  $G_j$  are distributed such that the corresponding EPSPs are measured from the resting potential obeying the lognormal distribution shown in (1).

Cortical excitatory synaptic transmissions are known to be mediated by two types of glutamatergic synaptic current, i.e., fast AMPA receptor-mediated currents ( $\tau_s \approx 2$ – $3$  ms) and slow NMDA receptor-mediated currents ( $\tau_s \approx 150$  ms). We note that, in our model, the excitatory synaptic current described by (3) only involves the AMPA current, but does not contain the NMDA current. The NMDA current is known to play a crucial role in activity-dependent modifications of synaptic conductance (synaptic plasticity) in hippocampal and neocortical circuits. Some models also suggest that the NMDA current is crucial for the generation of stable persistent neuronal firing [16] that is typically observed in working memory tasks, or spontaneous cortical activity [8] through reverberating synaptic input. However, as we will see later, the AMPA current is sufficient to maintain the stability of recurrent network activity under sparse synaptic distributions. To show this clearly, we do not include the NMDA current in our model.

Now we show that a lognormal weight distribution of excitatory synapses achieves aperiodic stochastic resonance on a single neuron receiving low-frequency spike inputs at individual excitatory and inhibitory synapses [Fig. 1(b)]. We measure the effect of stochastic resonance

by measuring the similarity between inputs to a group of very strong synapses and output spike trains of the postsynaptic neuron. In so doing, we vary the average membrane potential of the neuron by changing the rate of presynaptic spikes at weak-dense synapses, and calculate the cross-correlation coefficients (CCs) between output spikes and inputs to the strongest synapses. We find that CCs are maximized for input to the strongest synapse at a subthreshold membrane potential value that is about the midpoint between the resting potential and firing threshold. At more hyperpolarized levels, even an extremely strong EPSP ( $\sim 10$  mV) cannot evoke a postsynaptic spike, whereas at more depolarized levels, the neuron can fire without strong inputs. Here an interesting fact is that stochastic resonance does not work for a Gaussian distribution with the same mean and variance of the lognormal distribution [dotted-dashed line in Fig. 1(c)], uncovering the advantage of SSWD connections.

We can calculate the CC between input spike at strong synapses and output spike trains as

$$\begin{aligned} CC &= \frac{\langle x_{\text{in}}(t)x_{\text{out}}(t) \rangle - \langle x_{\text{in}}(t) \rangle \langle x_{\text{out}}(t) \rangle}{\sqrt{(\langle x_{\text{in}}(t)^2 \rangle - \langle x_{\text{in}}(t) \rangle^2)(\langle x_{\text{out}}(t)^2 \rangle - \langle x_{\text{out}}(t) \rangle^2)}} \\ &= Pr(x_{\text{out}}|x_{\text{in}}) \sqrt{\frac{r_{\text{in}}}{r_{\text{out}}}} \end{aligned} \quad (4)$$

by assuming that spike trains obey a low-rate Poisson process. Here,  $r_{\text{in}}$  and  $r_{\text{out}}$  are the firing rate of input and output sequences, respectively, and  $Pr(x_{\text{out}}|x_{\text{in}})$  is the conditional probability of an output spike for a given input spike at strong synapses. In numerical simulation, we evaluated  $Pr(x_{\text{out}}|x_{\text{in}})$  by detecting a postsynaptic spike within the epoch of EPSP rise from the arrival of an input spike. We can calculate  $Pr(x_{\text{out}}|x_{\text{in}})$  from the stationary probability density of the membrane potential  $P(v)$  obtained by analytically solving the Fokker–Planck equation of the membrane potential driven by the noise generated by weak-dense synapses. Namely, the conditional probability  $P_i$  of having an output spike given input to the  $i$ th strong synapse is equal to the area of the stationary density function satisfying  $v + E_{e,i}(v) \geq v_{\text{thr}}$ , where  $E_{e,i}(v)$  is the effective amplitude of EPSP measured from the average membrane potential. By solving the lower bound for the integration, we can obtain

$$P_i = \int_{\frac{(V_E - V_I)V_{\text{thr}} - \beta E_i V_E}{(V_E - V_L) - \beta E_i}}^{V_{\text{thr}}} P(v) dv \quad (5)$$

where the analytic expression of  $P(v)$  is found in [11]. The expression given in (5) is valid for an arbitrary strong synapse. Thus, we can obtain the theoretical curve of cross correlation [dashed line in Fig. 1(c)] by substituting  $P_i$  of the strongest synapse into  $Pr(x_{\text{out}}|x_{\text{in}})$  in (4). In the above theoretical treatment, the division of weak and strong

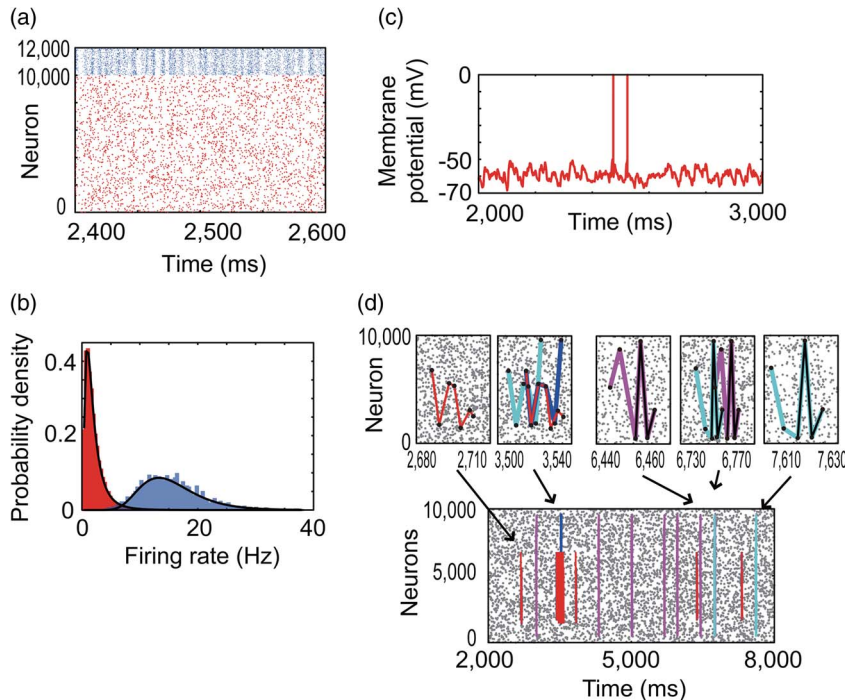


**Fig. 2.** Spontaneous activity in an SSWD network. Modified from [11]. (a) Spike raster is shown for an SSWD network of 10 000 excitatory (red) and 2000 inhibitory (blue) cells. The weights of excitatory synapses obey a lognormal distribution. (b) Distributions of firing rates are shown for excitatory and inhibitory neural populations. (c) A typical example of the fluctuating membrane potential of an excitatory neuron. (d) Spontaneous activity of the SSWD network contains many sequences propagating through strong synaptic pathways gated by stochastic resonance.

synapses remains somewhat arbitrary because the theory does not give a method to perform this division in a self-consistent manner. Therefore, we determined this division through numerical simulations, and found that the theoretical curve best coincided with numerical results when we divided 1000 excitatory synapses on a neuron into the five strongest synapses and the remaining weak synapses.

### III. ACTIVE NOISE GENESIS IN RECURRENT CIRCUITS

In Section II, we showed that experimentally observed lognormal weight distributions enable single neurons to respond reliably to spike inputs at strong synapses with the help of stochastic resonance emergent from the noise generated by massive inputs to weak synapses. We further show that a similar stochastic resonance effect occurs consistently on neurons embedded in a recurrent network. In the following, we show two such examples.

#### A. SSWD Recurrent Networks Modeling Spontaneous Cortical Activity

The above stochastic resonance effect on single neurons is by itself an interesting example of the benefit of noise in biological systems. However, whether cortical

neurons are dynamically set at the optimal noise level in a recurrent network is a highly nontrivial issue. We can show that this is indeed the case in SSWD neural networks. To see this, we conduct numerical simulations of a recurrent network model of 10 000 excitatory and 2000 inhibitory neurons that are randomly connected with coupling probabilities of excitatory and inhibitory connections being 0.1 and 0.5, respectively. Excitatory-to-excitatory connections obey the EPSP distribution shown in (1). The details of the model are found in [11]. Initially, all neurons are silent in the resting state. We may apply brief external Poisson spike trains to some neurons to trigger spontaneous activity of the network. Then, the model sustains a stable asynchronous firing even in the absence of external input [Fig. 2(a)]. This spontaneous network activity emerges purely from reverberating synaptic input, is stable in a very low-frequency regime [Fig. 2(b): typically,  $1 \sim 2$  spikes/s], and is highly irregular (the average coefficient of variation  $\sim 1$ ). All these properties are consistent with the spontaneous activity observed in cortical neurons [17].

Importantly, the reverberating synaptic input generated in the SSWD network maintains the average values of the membrane potentials of excitatory neurons at around  $-60$  mV [Fig. 2(c)], at which we show that the spike transmission at strong-sparse synapses becomes most

reliable [Fig. 1(c), shaded area]. In this state, massive inputs to weak-dense synapses depolarize the average subthreshold membrane potential, on top of which inputs to strong-sparse synapses may induce sparse spiking. Then, these spikes are distributed to weak synapses on some neurons to produce noise fluctuations in their membrane potentials. A characteristic feature of the SSWD network is that the same spikes propagate through multiple pathways mediated by strong synapses, generating multiple sequences in spontaneous activity [Fig. 2(d)]. Noise genesis by weak-dense synapses is necessary to keep the efficiency of this spike transmission at strong synapses optimal. Thus, weak-dense and strong-sparse synapses cooperate with each other for generating stable ongoing activity. Whether computation in cortical circuits relies on asynchronous irregular firing or spike sequences has been debated. Our model suggests the possibility that they are different, inseparable aspects of the same network mechanism.

### B. Stability of Sparse Spontaneous Activity

The maintenance of dynamical stability is a fundamental problem, when considering the spontaneous activity in recurrent neural network models. Therefore, we studied the conditions on network parameters to ensure the stability of the SSWD network model with of leaky-integrate-fire neurons. We can perform the stability analysis by means of the mean-field approximation [11]. The results of this theoretical analysis revealed that spontaneous activity in the SSWD network is stable only when excitatory-to-excitatory synaptic connections on average show longer delays than inhibitory-to-inhibitory synaptic connections. It is, therefore, important to inhibit a postsynaptic neuron slightly before excitatory synaptic inputs arrive at the neuron to keep an excitation–inhibition balance in the SSWD network. It is noted that this condition on synaptic delay may be loosened if we use a different mathematical model of spiking neurons, such as adaptive leaky integrate-and-fire neuron models that self-control the excitability, depending on the recent history of neuron’s activity [18].

A similar recurrent network model was proposed for the hippocampal CA3 circuit [8]. This recurrent network model uses a slow NMDA current to achieve stable spontaneous firing. We expected that the slow NMDA current would improve the stability of our network model. However, our results demonstrate that NMDA receptors are not necessary for the stability of spontaneous reverberating activity in recurrent networks with lognormal connections.

### C. Associative Memory SSWD Recurrent Network

The hippocampus is known to be crucial for episodic memory processes in the brain. In particular, hippocampal CA3 has sparse recurrent connections, and after pioneering work by Hopfield [19], [20] on associative memory (AM) network models, the CA3 circuit has been hypoth-

esized to be an attractor network for retrieving memorized activity patterns from disturbed cues for stored memory. This pattern completion hypothesis is now well supported by experiments [21]. It was recently shown that the local circuit of hippocampal CA3 has a lognormal distribution of synaptic conductance with a long tail [8]. We show that active noise genesis by lognormal weight distributions and the resultant stochastic resonance effect produces a good performance of attractor neural networks in memory retrieval.

Properties of pattern completion, such as storage capacity and memory retrieval dynamics, have been extensively studied in the statistical mechanics of the Hopfield AM network and its variants [22]–[27]. AM models of spiking neurons have been also studied, but their performance in memory storage is generally not so good as that of models with binary or analog neurons [28]–[37]. We construct AM network models of spiking neurons with lognormal weight distributions of recurrent connections to show that such distributions can generate internal noise useful for the retrieval of an embedded memory pattern [38].

We briefly explain how we embed  $p$  random binary patterns of 0 and 1  $\{\xi_i^\mu\}_{i=1,2,\dots,N_E}^{1,2,\dots,p}$  into excitatory-to-excitatory connections obeying a lognormal weight distribution on each postsynaptic neuron. We created sparse random patterns according to

$$\text{Prob}[\xi_i^\mu = 1] = a \quad \text{Prob}[\xi_i^\mu = 0] = 1 - a \quad (6)$$

where sparseness  $a$  obeys  $0 < a < 1$  and constraint  $\sum_i \xi_i^\mu = aN_E$  to suppress the nonhomogeneity across different memory patterns. If  $a$  is sufficiently small, neurons are activated only sparsely in each memory pattern. Conventionally, the weight matrix of the AM network model is determined by the local Hebbian rule, to which each memory pattern contributes the product of presynaptic and postsynaptic neural activities to synaptic connections and the contributions from multiple patterns are superimposed linearly:  $T_{ij} = \sum_{\mu=1}^p \xi_i^\mu \xi_j^\mu + \zeta_{ij}$ . Here, the second term  $\zeta_{ij} \in [0, 1)$  is an analog-valued random variable to make the distribution of  $T_{ij}$  continuous [35], [37]. This term is absent from the conventional AM models, but it is introduced here for the genesis of spontaneous activity specifically in networks storing only a small number of memory patterns. Information about the stored memory patterns is represented in the relative magnitudes of the elements of the connection matrix. Therefore, when we create a continuous connection matrix obeying a lognormal distribution, we should refer to this information as much as possible. Therefore, we determine the values of EPSP  $V_{ij}$  between excitatory neurons  $i$  and  $j$  so that the cumulative frequency of  $V_{ij}$  may coincide with that of  $T_{ij}$  [Fig. 3(a)]. In a lognormally connected network, we have to suppress the presence of hub neurons sending many connections to other neurons.

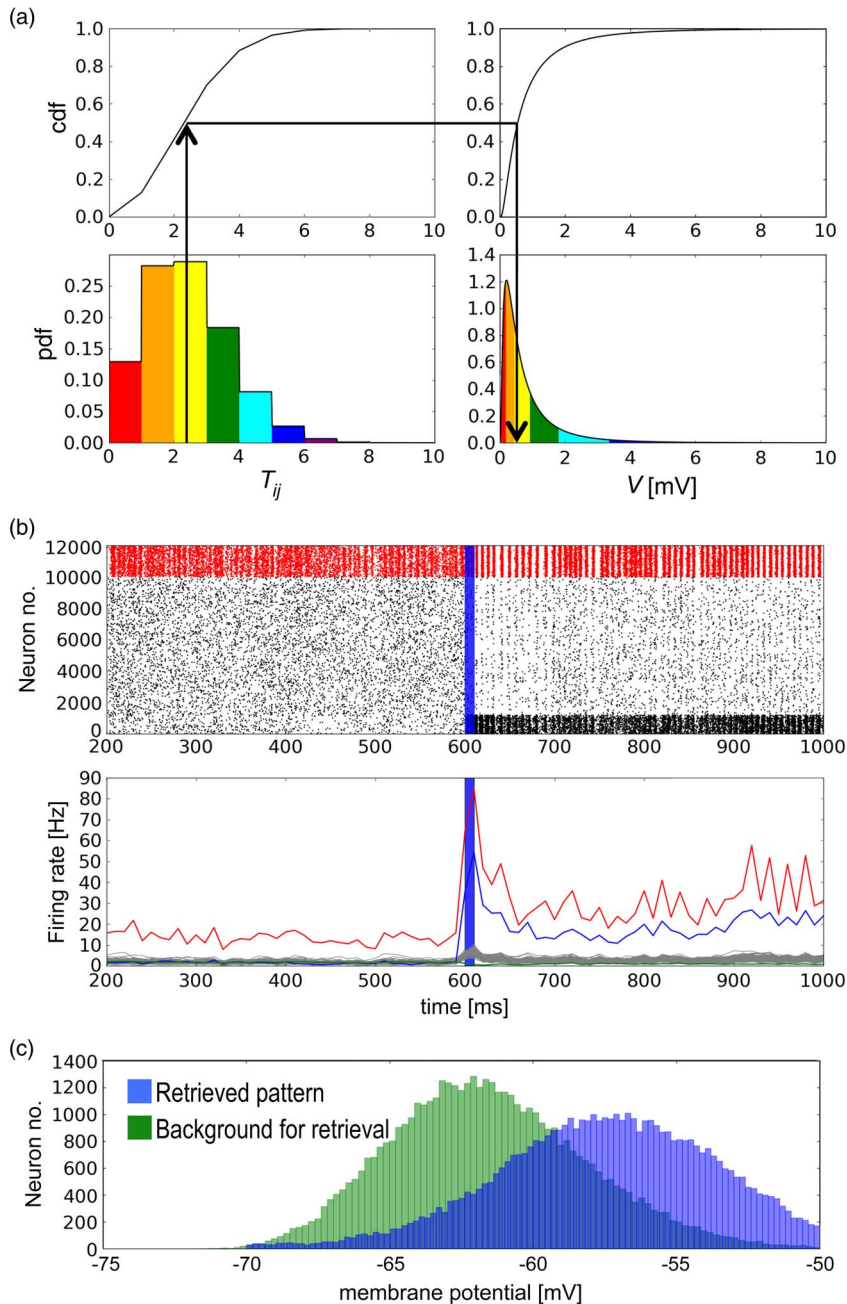


**Fig. 3.** Memory recall in an SSWD AM model. Modified from [38]. (a) A lognormal Hebbian connection matrix (right) was constructed from the standard Hebbian connection matrix (left). Lower panels show the distributions of the corresponding matrix elements, and the upper panels show their cumulative distributions. (b) Spike raster (upper) and the evolution of mean firing rates (lower) is shown. At time 600 ms, an external cue (blue) was applied to retrieve a memorized pattern 1. (c) Distributions of the membrane potential over neurons encoding pattern 1 (blue) and nonencoding (green) neurons.

We should also eliminate strong reciprocal connections and triangle network motifs to avoid high-frequency burst firing in some neurons. These details are explained in [38].

Numerical simulations reveal several interesting dynamical features of the model. The network is able to

sustain spontaneous activity at low firing rates without external input. If neurons encoding memory pattern 1 are stimulated by a brief cue signal, the model changes its dynamic behavior from spontaneous activity to a retrieval state, in which the average firing rates of the encoding neurons are much higher than those of nonencoding

neurons [Fig. 3(b)]. The distribution of the subthreshold membrane potentials is more depolarized or more hyperpolarized in the encoding and nonencoding neurons, respectively, which underlies the significantly different firing rates of the two groups [Fig. 3(c)]. As in other AM network models, this network model can retrieve a memory pattern successfully if the number of stored patterns is below a certain upper bound. It is interesting to compare the storage capacity (or the information capacity) between different AM models of spiking neurons even though a rigorous comparison is difficult. The storage capacity in general increases with the sparseness of memory patterns and decreases with the sparseness of synaptic connectivity. Parameter  $\alpha = (pa|\ln a|/c_E N_E)$  well characterizes such properties of AM networks with similar sparseness and network size. The value of this parameter is 0.036 ( $N_E = 10\,000$ ,  $c_E = 0.1$ ,  $a = 0.12$ ,  $p = 140$ ) in our model, 0.0058 ( $N_E = 8000$ ,  $c_E = 0.25$ ,  $a = 0.1$ ,  $p = 50$ ) in [35], and 0.0056 ( $N_E = 8000$ ,  $c_E = 0.2$ ,  $a = 0.05$ ,  $p = 60$ ) in [34]. Therefore, our model suggests that lognormal weight distributions significantly improve the storage capacity of spiking neurons.

The memory load also has a lower critical value below which spontaneous firing turns unstable, meaning that the network spontaneously evolves into one of the memory states without a cue signal. Unstable spontaneous firing states at a low level of the memory load have also been known in previous models [34]. It has been also pointed out that the Hebbian component should be sufficiently small to maintain stable spontaneous firing [35], [37]. The instability of spontaneous firing states shown at a very low memory load seems to be a common feature of the AM networks of spiking neurons with a Hebbian connection matrix. Altogether, the present model can perform the AM function at an intermediate level of memory load between the upper and lower critical values.

#### IV. ACTIVITY-DEPENDENT MECHANISMS FOR LOGNORMAL WEIGHT DISTRIBUTIONS

Biological mechanisms to realize the lognormal amplitude distribution of EPSPs remain unclear at present. Synaptic plasticity, however, is a promising candidate for the underlying mechanism, and several Hebb-like learning rules have been proposed. Here, Hebb-like learning rules refer to any learning rule that modifies synaptic weights depending on both presynaptic and postsynaptic neural activities.

##### A. Rate-Dependent Plasticity Mechanisms

The model proposed by Koulakov *et al.* is an extension of the conventional Hebbian learning rule using a multiplicative rather than additive synaptic growth rate [39]. In this model, the rate of weight modification  $dW_{ij}/dt$

for a synapse from neuron  $j$  to  $i$  depends on the product of postsynaptic and presynaptic firing rates  $f_i$  and  $f_j$  and the current value of synaptic strength  $W_{ij}$  as

$$\frac{dW_{ij}}{dt} = \epsilon_1 f_i^\alpha W_{ij}^\beta f_j^\gamma - \epsilon_2 W_{ij}.$$

Thus, the first term with coefficient  $\epsilon_1$  represents the rate of multiplicative and nonlinear weight growth. Exponents  $\alpha$ ,  $\beta$ , and  $\gamma$  characterize the nonlinear dependence of synaptic plasticity on  $f_i$ ,  $W_{ij}$ , and  $f_j$ , respectively. The second term with coefficient  $\epsilon_2$  is a passive linear decay of the synaptic strength. Assuming a linear neuron model as

$$f_i = \sum_j W_{ij} f_j,$$

Koulakov *et al.* showed that the learning rule successfully generates a lognormal distribution for  $W_{ij}$  if values of the coefficients are properly chosen such that the sum of exponents  $\alpha + \beta$  may be close to, but slightly smaller than, unity (e.g., 0.8). Remarkably, besides the lognormal distribution of EPSP amplitudes, the proposed learning rule concurrently gives a lognormal distribution of firing rate over neural population, which is another interesting example of lognormal distributions found in the brain [40], [41]. An experimentally testable prediction of the rate-based mechanism is that the weights of synapses terminating on a given neuron are correlated, but the average synaptic weights on individual neurons are widely distributed. Though this prediction has not been proved physiologically, advanced imaging techniques using voltage-sensitive fluorescent protein [42] may enable direct measurements of such correlations within and distributions over cortical neurons in the future.

##### B. Basic Properties of Spike-Timing-Dependent Plasticity

Spike-timing-dependent plasticity (STDP) modifies the weight (or strength) of synaptic connections between neurons depending on the relative timing of spike firing of postsynaptic and presynaptic neurons [9]. Though different forms of timing dependence (time window functions) are known for different types of synapses and neurons, the well-studied class of STDP describes Hebbian excitatory synapses with asymmetric time window functions. Namely, a synapse is potentiated (depressed) if the postsynaptic neuron fires earlier (later) than the induction of EPSP by a presynaptic spike input to the synapse. It is known that when the weight update rule does not depend on the weight (additive STDP), the dynamics of weight update is unstable, separating strong synapses and weak synapses further apart [Fig. 4(a)]. Therefore, the asymmetric Hebbian STDP gives rise to strong competition among excitatory synapses. The unstable synaptic dynamics of additive STDP, however, is theoretically problematic because it requires hard boundaries to maintain synaptic

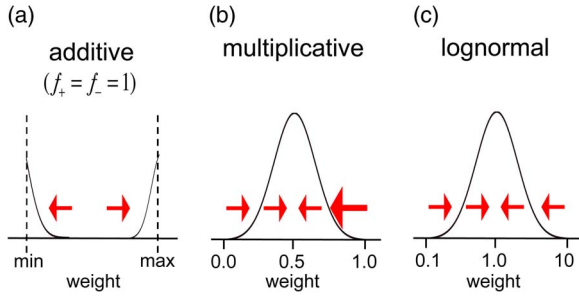


**Fig. 4. Synaptic dynamics in the three STDP models. Evolution of synaptic weights on a neuron receiving Poisson inputs is schematically illustrated for (a) additive, (b) multiplicative, and (c) lognormal STDP models.**

weights within a finite positive value range. The unstable dynamics also makes a flexible reorganization of synapses difficult when external inputs change their spatio-temporal structure.

Physiology has shown that the weight update of STDP not only depends on the window function, but also on the current magnitudes of synaptic weights [43]. The weight dependence was shown for excitatory synapses in the hippocampus (excitatory projections from CA3 to CA1). According to this rule, long-term potentiation (LTP) shows only weak or no weight dependence, but long-term depression (LTD) shows strong weight dependence: synaptic weight is reduced in proportion to the current magnitude of the weight. Thus, the total amplitude of weight update depends on the multiplication of the temporal component determined by the timing window function and the weight-dependent component, and the direction of weight update is determined by the relative timing between presynaptic and postsynaptic spikes. Due to the weight dependence, the dynamics of weight update is stable in multiplicative STDP, which is a virtue of the multiplicative rule. However, because stronger synapses undergo stronger depression, it is difficult to develop strong synapses and synaptic weights obey a Gaussian distribution, implying that synaptic weights are not specialized for the structure of synaptic input [Fig. 4(b)].

### C. STDP for the Generation Mechanism of Lognormal Weight Distributions

Log-STDP is a phenomenological STDP rule to generate a lognormal weight distribution of excitatory synapses when they receive uncorrelated Poisson spike trains [44]. We can derive log-STDP from multiplicative STDP by modifying the linear weight dependence of synaptic depression. In log-STDP, LTD exhibits linear weight dependence for weak synapses, but does not show strong weight dependence for large synaptic weights.

Thus, the weight dependence of log-STDP is represented by the following scaling factor to the weight update:

$$f_+(J) = c_+ \exp(-J/J_0 B)$$

$$f_-(J) = \begin{cases} \frac{c_- J}{J_0}, & \text{for } J \leq J_0 \\ c_- \left(1 + \frac{1}{\alpha} \ln(1 + \alpha(J/J_0 - 1))\right), & \text{for } J > J_0 \end{cases}$$

where  $f_+$  is for LTP and  $f_-$  for LTD. As mentioned above,  $f_+$  and  $f_-$  for  $J \leq J_0$  are almost identical to multiplicative STDP rule [43], and the key feature of log-STDP is the sublinear saturation of  $f_-$  for large values of  $J$ . Parameter  $\alpha$  characterizes the log-like saturation of the LTD component, and parameter  $\beta$  is chosen such that the function  $f_+$  may be approximately constant around  $J_0$  and exhibits an exponential decay only for values of  $J$  much larger than  $J_0$ . Weak LTD for strong synapses allows synaptic weights to grow, generating a long tail in the synaptic weight distribution [Fig. 4(c)].

A virtue of log-STDP is its sensitivity to correlated spike inputs. Though the detection of correlated spike inputs by STDP has been already known for additive STDP, correlated inputs drive excitatory synapses toward the tail of weight distribution in a graded manner, and this graded competition between synapses allows log-STDP to detect and analyze the relative strength of input correlations more effectively than additive or multiplicative STDP. For example, log-STDP can perform the principal component analysis (PCA) of the correlation structure of input spike trains (Fig. 5) [45].

Log-STDP solves the previously mentioned dilemma of additive and multiplicative STDP models between the stability of synapses and their functional specialization. To this end, log-STDP uses the long tail of weight distributions. Stable dynamics of synaptic modifications is possible because the scaling factors for both LTP and LTD saturate and the two competing effects are balanced on the long tail. Moreover, strong synapses tend to remain strong if input spike correlations are unchanged. However, once the input correlation structure changes, log-STDP adequately changes the weights of the individual synapses to adapt to the new configuration, achieving a robust functional specialization of synapses in the space of spike correlations. Thus, log-STDP may work better in a correlation-based neural code than in a rate-based code. However, we have to remember that the sensitivity of STDP to the firing rate depends on several factors, such as triplet interactions between presynaptic and postsynaptic spikes. An abstract generalization of STDP with nonlocal causality was also shown to generate approximately lognormal weight distributions [46].

### D. Other Mechanisms

We discuss yet another model that realizes the lognormal distribution of EPSP amplitudes based on an



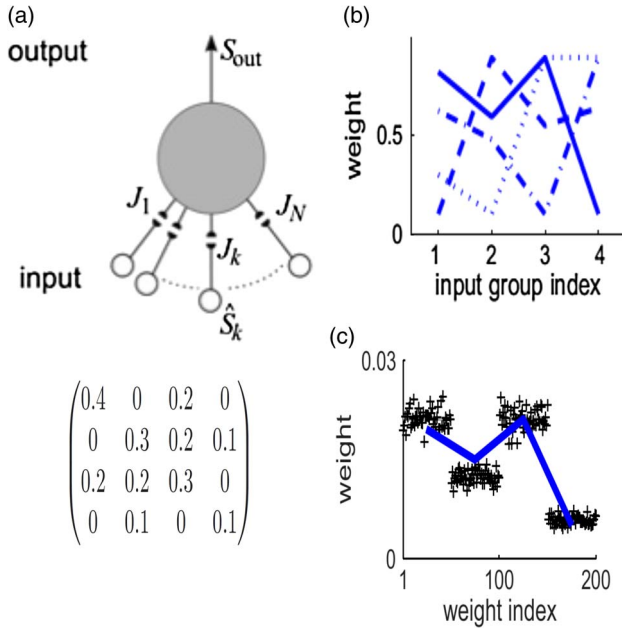


**Fig. 5. PCA of input correlation structure by log-STDP. Modified from [45]. (a)** Suppose that a neuron receives four groups of synaptic inputs that are correlated within and between the groups, with the pairwise correlation matrix shown below. **(b)** The principal components of input spike trains are obtained from the correlation matrix. **(c)** Log-STDP reorganizes the configuration of synaptic weights approximately in the direction of the first principal component. This nearly optimizes its detection capability.

additive Hebbian learning rule. As in Koullakov's approach, this learning rule can also explain the lognormal distributions of EPSP amplitudes and firing rates.

Before providing details, we note that spontaneous activity in the SSWD network model exhibits a long-tailed, actually lognormal, distribution of firing rates, as shown in Fig. 2(b). We can understand the origin of this lognormal distribution in almost the same way as discussed in [47]. Because each neuron in the network receives a large number of approximately independent identical spike inputs, the sum of these inputs is well described by a Gaussian distribution as a result of the central limit theorem. The sum of inputs determines the output firing rate of each neuron through the response function or the  $f - I$  curve of neurons. In a low-firing-rate regime, which holds for the spontaneous activity of the network model, the response function of leaky integrate-and-fire neurons is well approximated as

$$f \propto \frac{\theta - I}{\sigma} \exp\left(-\frac{(\theta - I)^2}{\sigma^2}\right)$$

where  $\theta$  and  $\sigma$  are parameters characterizing the firing threshold and the strength of input fluctuations, respectively [48]. Substituting  $I = I_0 + \Delta I$ , where  $I$  is the mean

and  $\Delta I$  is the deviation, and expanding the above expression with respect to  $\Delta I$ , we obtain

$$f \propto \exp\left(-2\frac{(\theta - I)}{\sigma^2}\Delta I\right).$$

Because  $\Delta I$  obeys a Gaussian distribution, the logarithm of firing rate  $\log f$  also obeys a Gaussian distribution, implying that the firing rate  $f$  obeys a lognormal distribution.

We note that the above derivation of the lognormal distribution of firing rates does not assume the lognormal distribution of EPSP amplitudes on each neuron. Therefore, the two distributions are essentially unrelated, and the lognormal distribution of firing rate arises without the lognormal distribution of EPSP amplitudes. This implies that if the network has a certain mechanism to relate the lognormal firing-rate distribution to the distribution of EPSPs, we can explain the latter lognormal distribution consistently. The following Hebbian synaptic plasticity rule provides such a mechanism:

$$\frac{dW_{ij}}{dt} = \varepsilon_1 f_i f_j - \varepsilon_2 W_{ij}.$$

In fact, in the steady solution  $W_{ij} \propto f_i f_j$ , the synaptic weight  $W_{ij}$  obeys a lognormal distribution because the product of lognormally distributed variables, i.e.,  $f_i f_j$ , again obeys a lognormal distribution. This mechanism is schematically illustrated in Fig. 6. Extending the learning rule to a spike-based rule and implementing it in a recurrent network model are interesting future problems.

## V. ATTEMPTS TOWARD NEUROMORPHIC ENGINEERING

Neuromorphic engineering is an attempt to construct electronic hardware models of the brain by realizing various functional properties of neurons and synapses on hardware chips. Despite recent progresses in nanoscale manufacturing technologies, large-scale neuromorphic hardware systems bear the tradeoff between detail level and required chip resources. Because the number of recurrent synapses typically scales as  $O(N^2)$  in a network of  $N$  neurons, having a good hardware model of synapses is of particular importance for solving this tradeoff. In other words, an effective solution to save resources on chips is to reduce the detail level of synapses. Recently, a hardware system that offers a 4-b resolution of synaptic weights modifiable with discretized STDP has been developed [13]. While a benchmark of this synapse model indicates that the resolution of synaptic weights is already useful for large-scale network simulations, it is unclear whether the same resolution is also useful for simulations of an SSWD recurrent network. At a first glance, the low resolution of synaptic weights makes it hard to effectively sample a long-tailed weight distribution.

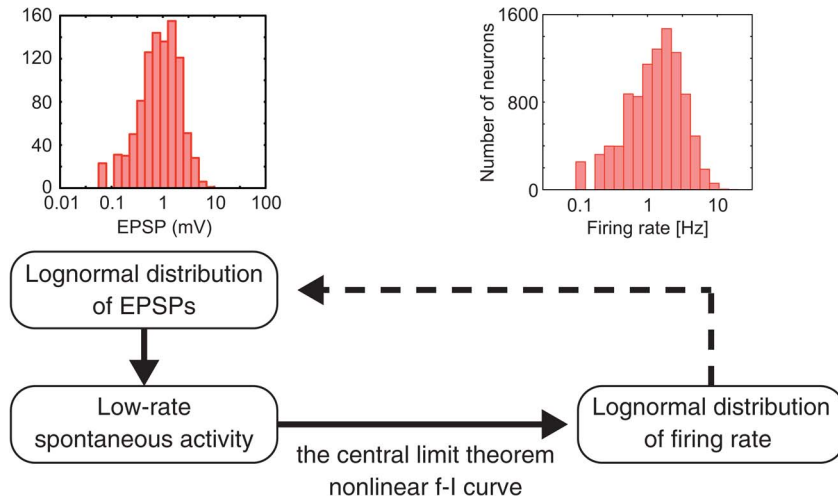


**Fig. 6. Mechanism to generate lognormal distributions. Low-rate spontaneous activity generates the lognormal distribution of EPSPs (upper left), which in turn gives the lognormal distribution of firing rates (upper right) through a rate-based Hebbian learning rule.**

We discretize a lognormal weight distribution in an  $n$ -bit resolution up to the maximum value  $J_{\max}$ . We set the discretized weight value of each synapse in the network at the midvalue of the corresponding bin. If the weight of some synapse is greater than  $J_{\max}$ , we set the discretized value to  $J_{\max}$ . Therefore, all synaptic weights stronger than  $J_{\max}$  are identified in the discretized model. Fig. 7(a) and (b) shows two examples of large-scale network simulations for  $n = 3$ ,  $J_{\max} = 16$  mV and  $n = 4$ ,  $J_{\max} = 12$  mV, respectively, demonstrating that both models can generate spontaneous network activity. However, the spiking pattern of neural population as well as the distributions of firing rate and firing irregularity differ significantly from experimental observations in the former model. Therefore, 4 b may be the minimal requirement for discrete synapses to obtain a natural firing pattern of cortical neurons.

## VI. FUTURE DIRECTIONS

In neuromorphic engineering, using most of the discretized weight values to represent weak-dense synapses is evidently a strong restriction on the capacity of information representation by SSWD networks. However, some experiments claim that cortical synapses are binary [49], and models are known that create useful computations with binary synapses [50]. The resolution of strong synapses necessary for efficient neural computation remains to be clarified. It is also an interesting question whether long-tailed distributions of synaptic weights add novel features to computation by a single neuron with complex morphological structure—the properties of biological neurons that have been largely ignored in engineering applications. In reality, the EPSP amplitude

measured in a neuron pair may represent the net strength of multiple synaptic contacts between the presynaptic and postsynaptic neurons. In such a situation, the spatial distribution of lognormal synapses on the dendrites may significantly influence signal transmission between neurons. In fact, stochastic resonance-like effects were revealed in morphologically realistic neuron models responding to brief changes in correlations among distributed noise sources [51]. However, several mechanisms are known in cortical neurons to counteract the distance-dependent filtering and attenuation of signal propagation along the dendrites [52], [53]. These mechanisms work to equalize the influences of distal and proximal synapses on somatic voltage, and may ensure the validity of the present results in networks of morphological neurons.

In a Hopfield model, the attenuation of strong recurrent signals, typically with the use of nonmonotonic response functions, is known to drastically improve the storage capacity [25], [54], [55], which would contradict the main claim of this paper. In Hebb's learning rule, strong synapses arise from the sum of correlated presynaptic and postsynaptic activities that occur in many memory patterns. This implies that the activation of strong synapses may coactivate neurons encoding different patterns, thus increasing crosstalk noise between different memory states. The attenuation of strong synaptic inputs by a nonmonotonic response function suppresses the crosstalk noise while preserving sufficiently strong signals to retrieve memory patterns. Taking this lesson into account, we would expect a further improvement of storage capacity in our model if we constructed lognormal synaptic weights after eliminating an adequate amount of strong synapses from the conventional Hebbian synaptic

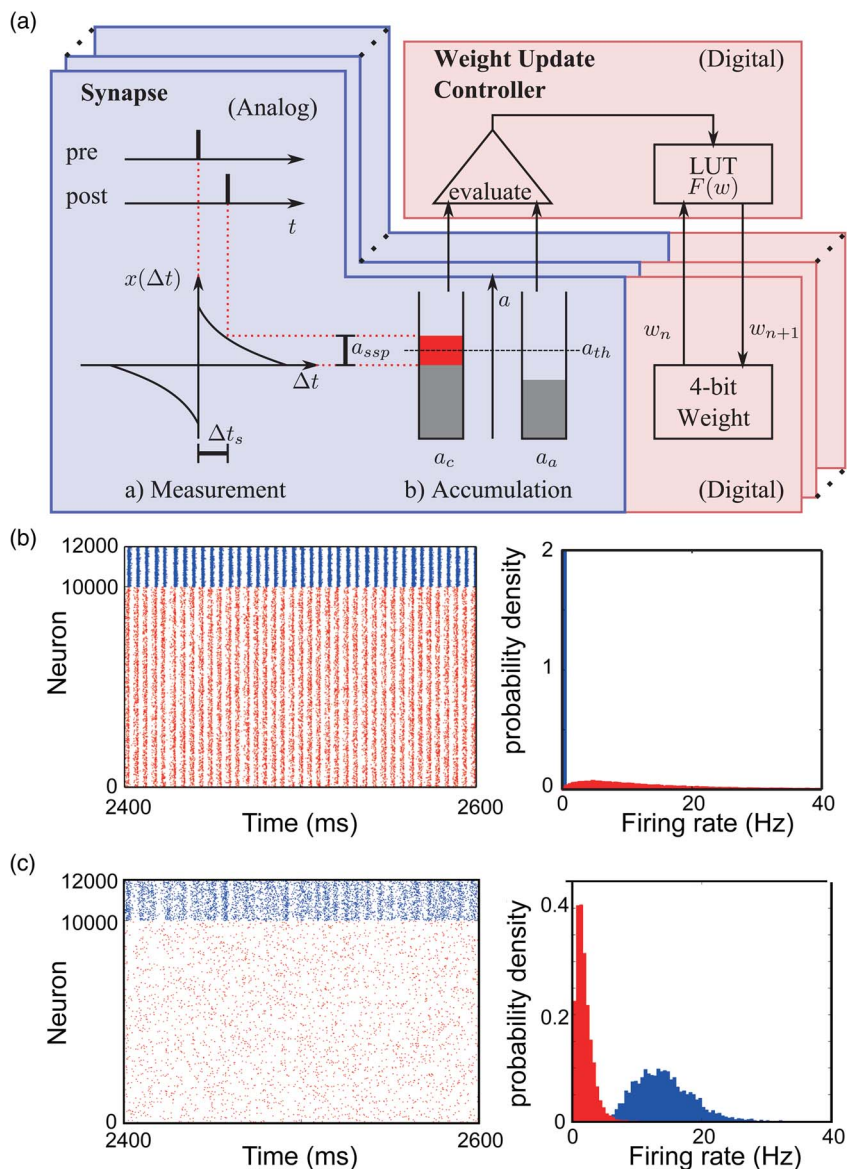


**Fig. 7. SSWD networks in neuromorphic engineering. (a) Schematic illustration of a 4-b model of modifiable synapses is replicated from [5]. (b) Spike raster (upper) and firing-rate distribution (lower) for 3-b lognormally distributed synapses with the maximum weight of 16 mV. (c) Similar results shown for 4-b synapses with the maximum weight of 12 mV.**

matrix. Whether this really occurs is an interesting open question.

In summary, we conjoin two fundamental principles in signal processing and complex phenomena observed in cortical neural networks: stochastic resonance and noisy internal brain states. The key of this link is the coexistence of a spectrum of SSWD connections that gives a mechanism by which excitable networks generate and maintain optimal noise level for efficient spike communication. These results have implications for the role of noise in networks with a broad spectrum of coupling strengths, such as the gating of specific signal pathways with the

probabilities of pathway selection modulated by the dynamics of internal noise generation. We have shown that such internal noise enables AM models of spiking neurons to have relatively large storage capacity compared with the previous spiking network models. This result is interesting because it gives an example in which noise plays an active role in information processing, and because it proves that spiking neurons are much less effective than binary neurons as far as the capacity of AM is concerned. In particular, recent experiments have suggested that spontaneous cortical activity provides prior information for probabilistic inference, spontaneously cycling neural

activities associated with past experiences [56]. How such probabilistic computation may be implemented by lognormal weight distributions and related plasticity rules is an intriguing open question. ■

## Acknowledgment

The authors would like to thank T. Negoro for providing simulation data for neuromorphic engineering.

## REFERENCES

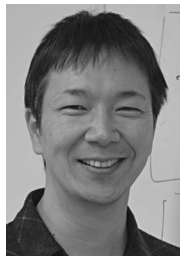
- [1] C. Holmgren, T. Harkany, B. Svennenfors, and Y. Zilberter, "Pyramidal cell communication within local networks in layer 2/3 of rat neocortex," *J. Physiol.*, vol. 551, pp. 139–153, 2003.
- [2] A. Stepanyants, G. Tamás, and D. B. Chklovskii, "Class-specific features of neuronal wiring," *Neuron*, vol. 43, pp. 251–259, 2004.
- [3] N. Kalisman, G. Silberberg, and H. Markram, "The neocortical microcircuit as a tabula rasa," *Proc. Nat. Acad. Sci.*, vol. 102, pp. 880–885, 2005.
- [4] Y. Yoshimura, J. L. M. Dantzker, and E. M. Callaway, "Excitatory cortical neurons form fine-scale functional networks," *Nature*, vol. 433, pp. 868–873, 2005.
- [5] R. Perin, T. K. Berger, and H. Markram, "A synaptic organizing principle for cortical neuronal groups," *Proc. Nat. Acad. Sci. USA*, vol. 108, pp. 5419–5424, 2011.
- [6] S. Song, P. J. Sjöström, M. Reigl, S. B. Nelson, and D. B. Chklovskii, "Highly nonrandom features of synaptic connectivity in local cortical circuits," *PLoS Biol.*, vol. 3, no. 3, 2005, e68.
- [7] S. Lefort, C. Tómm, J. C. Floyd Sarria, and C. C. H. Petersen, "The excitatory neuronal network of the C2 barrel column in mouse primary somatosensory cortex," *Neuron*, vol. 61, pp. 301–316, 2009.
- [8] Y. Ikegaya, T. Sasaki, D. Ishikawa, N. Honma, K. Tao, N. Takahashi, G. Minamisawa, S. Ujita, and N. Matsuki, "Interpyramid spike transmission stabilizes the sparseness of recurrent network activity," *Cereb. Cortex*, vol. 23, no. 2, pp. 293–304, 2013.
- [9] B. Barbour, N. Brunel, V. Hakim, and J. P. Nadal, "What can we learn from synaptic weight distributions?" *Trends Neurosci.*, vol. 30, no. 12, pp. 622–629, 2007.
- [10] L. Sarid, R. Bruno, B. Sakmann, I. Segev, and D. Feldmeyer, "Modeling a layer 4-to-layer 2/3 module of a single column in rat neocortex: Interweaving *in vitro* and *in vivo* experimental observations," *Proc. Nat. Acad. Sci. USA*, vol. 104, pp. 16353–16358, 2007.
- [11] J.-N. Teramae, Y. Tsubo, and T. Fukai, "Optimal spike-based communication in excitable networks with strong-sparse and weak-dense links," *Sci. Rep.*, vol. 2, 2012, DOI: 10.1038/srep00485.
- [12] J. Teramae, Y. Tsubo, and T. Fukai, "Long-tailed statistics of corticocortical EPSPs: Origin and computational role of noise in cortical circuits," in *Advances in Cognitive Neurodynamics (III)*. Amsterdam, The Netherlands: Springer-Verlag, 2013, pp. 161–167.
- [13] T. Pfeil, T. C. Potjans, S. Schrader, W. Potjans, J. Schemmel, M. Diesmann, and K. Meier, "Is a 4-bit synaptic weight resolution enough?—constraints on enabling spike-timing dependent plasticity in neuromorphic hardware," *Front. Neurosci.*, vol. 6, 2012, DOI: 10.3389/fnins.2012.00090.
- [14] N. Yasumatsu, M. Matsuzaki, T. Miyazaki, J. Noguchi, and H. Kasai, "Principles of long-term dynamics of dendritic spines," *J. Neurosci.*, vol. 28, pp. 13592–13608, 2008.
- [15] Y. Loewenstein, A. Kuras, and S. Rumpel, "Multiplicative dynamics underlie the emergence of the log-normal distribution of spine sizes in the neocortex *in vivo*," *J. Neurosci.*, vol. 31, pp. 9481–9488, 2011.
- [16] X. J. Wang, "Probabilistic decision making by slow reverberation in cortical circuits," *Neuron*, vol. 36, pp. 955–968, 2002.
- [17] A. Destexhe, M. Rudolph, and D. Paré, "The high-conductance state of neocortical neurons *in vivo*," *Nature Rev. Neurosci.*, vol. 4, pp. 739–751, 2003.
- [18] R. Jolivet, R. Kobayashi, A. Rauch, R. Naud, S. Shinomoto, and W. Gerstner, "A benchmark test for a quantitative assessment of simple neuron models," *J. Neurosci. Methods*, vol. 169, pp. 417–424, 2008.
- [19] J. J. Hopfield, "Neural networks and physical systems with emergent collective computational abilities," *Proc. Nat. Acad. Sci. USA*, vol. 79, pp. 2554–2558, 1982.
- [20] J. J. Hopfield, "Neurons with graded response have collective computational properties like those of two-state neurons," *Proc. Nat. Acad. Sci. USA*, vol. 81, pp. 3088–3092, 1984.
- [21] K. Nakazawa, M. C. Quirk, R. A. Chitwood, M. Watanabe, M. F. Yeckel, L. D. Sun, A. Kato, C. A. Carr, D. Johnston, M. A. Wilson, and S. Tonegawa, "Requirement for Hippocampal CA3 NMDA receptors in associative memory recall," *Science*, vol. 297, pp. 211–218, 2002.
- [22] D. J. Amit, H. Gutfreund, and H. Sompolinsky, "Spin-glass models of neural networks," *Phys. Rev. A*, vol. 32, pp. 1007–1018, 1985.
- [23] B. Derrida, E. Gardner, and A. Zippelius, "An exactly solvable asymmetric neural network model," *Europhys. Lett.*, vol. 4, pp. 167–173, 1987.
- [24] M. V. Tsodyks and M. V. Feigel'man, "The enhanced storage capacity in neural networks with low activity level," *Europhys. Lett.*, vol. 6, pp. 101–105, 1988.
- [25] M. Shiino and T. Fukai, "Self-consistent signal-to-noise analysis of the statistical behavior of analog neural networks & enhancement of the storage capacity," *Phys. Rev.*, vol. E48, pp. 867–897, 1993.
- [26] A. C. C. Coolen and D. Sherrington, "Dynamics of fully connected attractor neural networks near saturation," *Phys. Rev. Lett.*, vol. 71, pp. 3886–3889, 1993.
- [27] M. Okada, "A hierarchy of macrodynamical equations for associative memory," *Neural Netw.*, vol. 8, pp. 833–838, 1995.
- [28] W. Gerstner and J. L. Hemmen, "Associative memory in a networks of spiking neurons," *Network*, vol. 3, pp. 139–164, 1992.
- [29] A. Lansner and E. Fransén, "Modeling Hebbian cell assemblies comprised of cortical neurons," *Network*, vol. 3, pp. 105–119, 1992.
- [30] A. Treves, "Mean-field analysis of neuronal spike dynamics," *Network*, vol. 4, pp. 259–284, 1993.
- [31] W. Maass and T. Natschläger, "Networks of spiking neurons can emulate arbitrary Hopfield nets in temporal coding," *Network*, vol. 8, pp. 355–371, 1997.
- [32] D. J. Amit and N. Brunel, "Model of global spontaneous activity and local structured activity during delay periods in the cerebral cortex," *Cereb. Cortex*, vol. 7, pp. 237–252, 1997.
- [33] F. T. Sommer and T. Wennekers, "Associative memory in networks of spiking neurons," *Neural Netw.*, vol. 14, pp. 825–834, 2001.
- [34] M. Curti, G. Mongillo, G. L. Camera, and D. J. Amit, "Mean field and capacity in realistic networks of spiking neurons storing sparsely coded random memories," *Neural Comput.*, vol. 16, pp. 2597–2637, 2004.
- [35] P. Latham and S. Nirenberg, "Computing and stability in cortical networks," *Neural Comput.*, vol. 16, pp. 1385–1412, 2004.
- [36] Y. Aviel, D. Horn, and M. Abeles, "Memory capacity of balanced networks," *Neural Comput.*, vol. 17, pp. 691–713, 2005.
- [37] Y. Roudi and P. Latham, "A balanced memory network," *PLoS Comput. Biol.*, vol. 3, 2007, DOI: 10.1371/journal.pcbi.0030141.
- [38] N. Hiratani, J. N. Teramae, and T. Fukai, "Associative memory model with long-tail-distributed Hebbian synaptic connections," *Front. Comput. Neurosci.*, vol. 6, 2013, DOI: 10.3389/fncom.2012.00102.
- [39] A. A. Koulakov, T. Hromádka, and A. M. Zador, "Correlated connectivity and the distribution of firing rates in the neocortex," *J. Neurosci.*, vol. 29, pp. 3685–3694, 2009.
- [40] T. Hromádka, M. R. DeWeese, and A. M. Zador, "Sparse representation of sounds in the unanesthetized auditory cortex," *PLoS Biol.*, vol. 6, 2008, e16.
- [41] K. Mizuseki and G. Buzsáki, "Preconfigured, skewed distribution of firing rates in the hippocampus and entorhinal cortex," *Cell Rep.*, vol. 4.5, pp. 1010–1021, 2013.
- [42] T. Knöpfel, "Genetically encoded optical indicators for the analysis of neuronal circuits," *Nat. Rev. Neurosci.*, vol. 13, pp. 687–700, 2012.
- [43] M. C. W. van Rossum, G. Q. Bi, and G. G. Turrigiano, "Stable Hebbian learning from spike timing-dependent plasticity," *J. Neurosci.*, vol. 20, pp. 8812–8821, 2000.
- [44] M. Gilson and T. Fukai, "Stability versus neuronal specialization for STDP: Long-tail weight distributions solve the dilemma," *PLoS ONE*, vol. 6, 2011, e25339.
- [45] M. Gilson, T. Fukai, and A. N. Burkitt, "Spectral analysis of input spike trains by spike-timing-dependent plasticity," *PLoS Comput. Biol.*, 2012, e1002584.
- [46] A. Nathan and V. C. Barbosa, "Network algorithmics and the emergence of the cortical synaptic-weight distribution," *Phys. Rev. E*, vol. 81, no. 2, 2010, 021916.
- [47] A. Roxin, N. Brunel, D. Hansel, G. Mongillo, and C. van Vreeswijk, "On the distribution of firing rates in networks of cortical neurons," *J. Neurosci.*, vol. 31, pp. 16217–16226, 2011.
- [48] N. Brunel, "Dynamics of sparsely connected networks of excitatory and inhibitory spiking neurons," *J. Comput. Neurosci.*, vol. 8, pp. 183–208, 2000.
- [49] C. C. Petersen, R. C. Malenka, R. A. Nicoll, and J. J. Hopfield, "All-or-none potentiation at

- CA3–CA1 synapses,” *Proc. Nat. Acad. Sci. USA*, vol. 95, pp. 4732–4737, 1998.
- [50] A. Soltani and X. J. Wang, “Synaptic computation underlying probabilistic inference,” *Nature Neurosci.*, vol. 13, pp. 112–119, 2010.
- [51] M. Rudolph and A. Destexhe, “Correlation detection and resonance in neural systems with distributed noise sources,” *Phys. Rev. Lett.*, vol. 86, pp. 3662–3665, 2001.
- [52] J. C. Magee and E. P. Cook, “Somatic EPSP amplitude is independent of synapse location in hippocampal pyramidal neurons,” *Nature Neurosci.*, vol. 3, pp. 895–903, 2000.
- [53] V. Menon, T. F. Musial, A. Liu, Y. Katz, W. L. Kath, N. Spruston, and D. A. Nicholson, “Balanced synaptic impact via distance-dependent synapse distribution and complementary expression of AMPARs and NMDARs in hippocampal dendrites,” *Neuron*, vol. 80, pp. 1451–1463, 2013.
- [54] M. Morita, “Memory and learning of sequential patterns by nonmonotone neural networks,” *Neural Netw.*, vol. 9, pp. 1477–1489, 1996.
- [55] S. Ishii and M. Sato, “Associative memory based on parametrically coupled chaotic elements,” *Physica D, Nonlinear Phenomena*, vol. 121, pp. 344–366, 1998.
- [56] P. Berkes, G. Orbán, M. Lengyel, and J. Fiser, “Spontaneous cortical activity reveals hallmarks of an optimal internal model of the environment,” *Science*, vol. 331, pp. 83–87, 2011.

#### ABOUT THE AUTHORS

**Jun-nosuke Teramae** was born in 1974. He received the Ph.D. degree in physics from Kyoto University, Kyoto, Japan, in 2003.

After spending several years at the Laboratory for Neural Circuit Theory, Brain Science Institute, RIKEN, Saitama, Japan, as a Researcher and a Deputy Laboratory Head, he became an Associate Professor at the Graduate School of Information Science and Technology, Osaka University, Suita, Osaka, Japan, in 2012. His research interests include theoretical neuroscience, stochastic computation and signal processing in the brain, nonlinear physics of systems with fluctuations, machine learning, and the applications of all of them to various engineering problems.



**Tomoki Fukai** was born in Tokyo, Japan, in 1958. He graduated from the Department of Physics, Waseda University, Shinjuku, Tokyo, Japan, in 1980 and received the Ph.D. degree from the same university in 1985.

After two years of experiences as a visiting Fellow of the Theoretical Physics Group, Tata Institute, Mumbai, India, he was appointed an Associate Professor of Tokai University, Shibuya, Tokyo, Japan, in 1991, and then a Professor of the Information Communication Engineering Department and the Brain Research Center, Tamagawa University, Machida, Tokyo, Japan, in 2001. In 2005, he moved to the RIKEN Brain Science Institute (BSI), Wako, Saitama, Japan, as a team leader of the Laboratory for Neural Circuit Theory and the Director of the Theoretical Neuroscience Group. He has been a Senior Team Leader of BSI since 2010. The goal of his research is to understand how neural circuits in the brain, especially cortical circuits, compute quantities of interests with spikes. He approaches this goal by constructing neural network models and analyzing massively parallel neural data obtained in experiments.

